

Original Article

Cite this article: Villafañe PG, Cónsole-Gonella C, Citton P, Díaz-Martínez I, and de Valais S (2021) Three-dimensional stromatolites from Maastrichtian–Danian Yacoraite Formation, Argentina: modelling and assessing hydrodynamic controls on growth patterns. *Geological Magazine* **158**: 1756–1772. <https://doi.org/10.1017/S0016756821000315>

Received: 11 June 2020

Revised: 25 March 2021

Accepted: 26 March 2021

First published online: 29 April 2021





Keywords:

Intertidal stromatolites; Yacoraite Formation; Maastrichtian–Danian; palaeoenvironmental reconstruction; 3D modelling

Author for correspondence:

Patricio Guillermo Villafañe,
Email: pgvillafan@gmail.com

Three-dimensional stromatolites from Maastrichtian–Danian Yacoraite Formation, Argentina: modelling and assessing hydrodynamic controls on growth patterns

Patricio Guillermo Villafañe^{1,2,3}, Carlos Cónsole-Gonella^{1,3,4} , Paolo Citton^{1,5} , Ignacio Díaz-Martínez^{1,5}  and Silvina de Valais^{1,5} 

¹Consejo Nacional de Investigaciones Científicas y Técnicas (CONICET), Godoy Cruz 2290, PC C1425FQB, Ciudad Autónoma de Buenos Aires, Argentina; ²Laboratorio de Investigaciones Microbiológicas en Lagunas Andinas (LAMIR), Avenida Belgrano y Pasaje Caseros, San Miguel de Tucumán, PC 4000, Tucumán, Argentina; ³Instituto Superior de Correlación Geológica (INSUGEO, CONICET-Universidad Nacional de Tucumán), Avenida Presidente Peron s/n, Yerba Buena, PC 4107, Tucumán, Argentina; ⁴Institute of Paleontology, Hebei GEO University, 136 East Huai' an Rd, Shijiazhuang, Hebei PC 050031, China and ⁵Instituto de Investigación en Paleobiología y Geología (IIPG, CONICET-UNRN), Avenida Roca 1242, General Roca, PC R8332, Río Negro, Argentina

Abstract

Stromatolites are biogenic sedimentary structures formed by the interplay of biological (microbial composition) and environmental factors (local hydrodynamic conditions, clastic input and/or water chemistry). Well-preserved, three-dimensional (3D) fossil stromatolites are key to assessing the environmental factors controlling their growth and resulting morphology in space and time. Here, we report the detailed analysis of well-exposed, highly informative stromatolite build-ups from a single stratigraphic horizon within the Maastrichtian–Danian Yacoraite Formation (Argentina). This study focuses on the analysis of depositional processes driving intertidal to shallow subtidal stromatolites. Overall depositional architecture, external morphology and internal arrangement (mega, macro, meso and microstructures) of stromatolite build-ups were analysed and combined with 3D photogrammetric models, allowing us to decipher the links between stromatolite structure and tidal dynamics. Results suggest that external morphology and architecture of elongated and parallel clusters grew under the influence of run-off channels. The internal morphology exhibits columnar structures where the space between columns is interpreted as recharge or discharge channels. This work supports the theory that stromatolites can be used as a high-resolution tool in the assessment of water dynamics, and provides a new methodological approach and data for the dynamic reconstruction of intertidal stromatolite systems through the geological record.

1. Introduction

Stromatolites are laminated organo-sedimentary structures present in the geological record from 3.45 Ga, before the Cambrian explosion (Schopf, 1996; Grotzinger & Knoll, 1999; Reid *et al.* 2000; Allwood *et al.* 2006). These structures are considered microbial in origin and represent one of the earliest evidence of benthic microbial communities on Earth (Grotzinger & Knoll, 1999).

Stromatolites develop due to the complex interplay between biological (community structure) and environmental factors, such as exposure to water energy, water supply and drainage, input of clastic sediments and mineral precipitation rates (Golubic, 1976). However, near the coastline of peri-marine environments, the main extrinsic agents influencing the development of stromatolites are commonly related to wave intensity and tidal regimen (Logan *et al.* 1964; Gebelein, 1976; Andres & Reid, 2006; Suosaari *et al.* 2016a). Wave action and tidal oscillation control the accommodation space and, consequently, both the vertical and lateral distribution of stromatolites (e.g. Andres & Reid, 2006; Kah *et al.* 2006). Moreover, wave action and tidal oscillation influence both the external morphology (Dill *et al.* 1986; Reid & Browne, 1991; Jahnert & Collins, 2012) and the internal structure at various scales (Reid & Browne, 1991; Suosaari *et al.* 2016b). The investigation of growth processes in fossil stromatolites is therefore a key element for reconstructing palaeoenvironmental conditions during their formation and development.

The Maastrichtian–Danian Yacoraite Formation (Turner, 1959) represents a carbonate deposit widely distributed in northwestern Argentina and is an excellent marker horizon in the Salta Group. The main lithology of the formation is carbonate–calcareous and dolomitic, but it also contains shale and sandstone (Marquillas *et al.* 2005; Sánchez & Marquillas, 2010;

Deschamps *et al.* 2020). The Yacoraite Formation constitutes an epicontinental unit widely exposed in northwestern Argentina (Marquillas *et al.* 2005).

Stromatolites (microbialites) from the Yacoraite Formation were first reported in the late nineteenth century. Brackebusch (1883) mentioned the presence of domic stromatolites ('*Pucalithus*'), considered equivalent to the structures called '*calcaire ondulée*' by d'Orbigny (1842) in the Cretaceous strata of Bolivia. Over the years, several stromatolite deposits have been recognized from this geological unit, but only mentioned or briefly described and discussed in a regional palaeoenvironmental and sedimentological context (e.g. Marquillas, 1984, 1985; Palma, 1984; Marquillas & Salfity, 1989, 1994; Marquillas *et al.* 2003, 2005; Cónsole-Gonella *et al.* 2012, 2017; Cónsole-Gonella & Marquillas, 2014; Bunevich *et al.* 2017; Gomes *et al.* 2019; Deschamps *et al.* 2020).

Different stromatolitic morphologies were reported from intertidal facies of the Yacoraite Formation, such as isolated oncoids, planar-laminated stromatolites, isolated nodular stromatolites and moustache-like stromatolites (Hamon *et al.* 2012).

An excellent case study is represented by the shoreline carbonate lagoon deposits of Maimará locality, where three-dimensional (3D) preserved stromatolites are exposed. These stromatolites belong to facies classified as stromatolitic boundstone, in which they are related to siltstones, pelite layer, wackestone and erosive surfaces. Within this facies, hemispheroidal domes and semicircular dome morphologies were recognized. These levels have developed in a subtidal and/or lower intertidal to intertidal palaeoenvironment, with areas proximal to and more distant from the coastline, under wave and tide action and with variable depth and/or energy stages, as suggested by facies analysis (Cónsole-Gonella *et al.* 2017).

The main goal of this contribution is to characterize in detail the relationships between this stromatolite system and hydrodynamic factors, in order to reconstruct in detail the palaeoenvironment.

2. Geological context

The Yacoraite Formation belongs to the Balbuena Subgroup (Upper Cretaceous–lower Paleocene), which is the early post-rift unit of the Salta Group (Lower Cretaceous–Eocene), an intracontinental rift-type basin (e.g. Salfity & Marquillas, 1994; Marquillas *et al.* 2005). This basin is associated with a tectonic regional context of extensional type in NW Argentina, which is common in basins of similar age in the Central Andes and nearby regions (Marquillas *et al.* 2011). The Salta Group is represented in seven sub-basins of Salta and Jujuy provinces, Argentina, namely Tres Cruces, Lomas de Olmedo, Metán, Alemania (Reyes, 1972), El Rey (Salfity, 1980), Sey (Schwab, 1984) and Brealito (Sabino, 2002).

The Yacoraite Formation comprises the Cretaceous–Palaeogene (K–Pg) boundary, as indicated by the varying stratigraphy. In the Metán sub-basin (Salta province), the unit is Maastrichtian in age as indicated by U–Pb radiometric dating (Marquillas *et al.* 2011) of rock samples several metres below the top. In the Maimará locality, Sial *et al.* (2001) identified the K–Pg boundary, although its position in the stratigraphical section is not indicated. However, the overlying Tunal Formation is dated as Danian in age based on palynomorphs (Quattrocchio *et al.* 2000). On the basis of these data, the stromatolite levels within the Yacoraite Formation are interpreted as Maastrichtian in age, in a stratigraphic position likely close to the K–Pg boundary.

In the Maimará locality, the fossil record of the Yacoraite Formation is made up of gastropods, ostracods, fish remains,

vertebrate tracks, invertebrate trace fossils, microbialites (Díaz-Martínez *et al.* 2016; Cónsole-Gonella *et al.* 2017), and palynomorphs (Moroni, 1984). The studied stratigraphic section records a lagoon palaeoenvironment with tidal influence associated with supratidal bodies of ephemeral ponds, described by Cónsole-Gonella *et al.* (2017).

2.a. Stratigraphy

The studied outcrop (23° 37' 30.92" S, 65° 23' 56.07" W) is located at the Maimará locality, SE of the Quebrada de Humahuaca, Jujuy province (Fig. 1). Palaeogeographically, the area belongs to the austral sector of the Tres Cruces sub-basin, close to the Salta–Jujuy ridge, which confers basin edge features on the deposit and distinguishes it from the austral sectors of the Salta Group basin (see Salfity & Marquillas, 1994; Marquillas *et al.* 2005).

The Balbuena Subgroup (Maastrichtian–Danian) lies unconformably above the quartz sandstones of the Mesón Group (middle–upper Cambrian) and it is represented by the Lecho Formation (Maastrichtian) and the Yacoraite Formation (Maastrichtian–Danian) (Cónsole-Gonella *et al.* 2017) (Fig. 2). In the studied section, the Lecho Formation is represented by averaging 3 m of coarse to fine sandstones and angular, poorly sorted conglomerates immersed in a silty/sandy clay matrix, interpreted as the product of debris flows in a probably alluvial fan environment, with sparse water supply (Cónsole-Gonella *et al.* 2017). Above, the Yacoraite Formation has an average thickness of 42 m (Figs. 3, 4a) and is represented by tabular, well-stratified, fossiliferous limestones and calcareous sandstones, with thin intercalations of laminate mudstones and stromatolite levels (Cónsole-Gonella *et al.* 2017).

3. Methodology

The integrated section of the Balbuena Subgroup is based on Cónsole-Gonella *et al.* (2017) (Fig. 4a). The best preserved stromatolite level, which is the main object of this study, is MNE5 (Fig. 4b). Sedimentary structures, stratal geometry, boundaries, layering, thickness variations and fossil content were also described to build a detailed logged section. Ten samples were collected and currently housed in the Paleontología de Invertebrados Lillo collection (PIL17.150–17.160) of the Universidad Nacional de Tucumán (Argentina). Polished slabs and thin-sections were prepared, labelled and housed at the petrography laboratory of the Instituto Superior de Correlación Geológica (INSUGEO), Tucumán, Argentina (collection numbers PIL-MNE5-P and PIL-MNE5-T1–T5).

Stromatolites were described following a traditional multiscale approach (e.g. Preiss, 1976; Shapiro, 2000; Vennin *et al.* 2015), focused on the separate characterization of the megastructure (i.e. large-scale features of microbialite bed), macrostructure (i.e. gross form of microbialite bodies with typical dimensions of tens of centimetres to metres), mesostructure (i.e. internal textures of macrostructural elements visible to the naked eye) and microstructure (i.e. microscopic fabrics observed under petrographic analysis).

The external morphology and architecture of stromatolites was determined on the basis of field and laboratory data, including dimensions and spatial distribution, overall external appearance, colour, types of contacts and stratal thicknesses. The description is based on the proposals by Cumings (1932), Clarke & Teichert (1946), Logan (1961), Aitken (1967) and Gebelein (1976). More recent concepts discussed by Davaud *et al.* (1994), Nehza & Woo (2006), Forbes *et al.* (2010), Jahnert & Collins (2012),

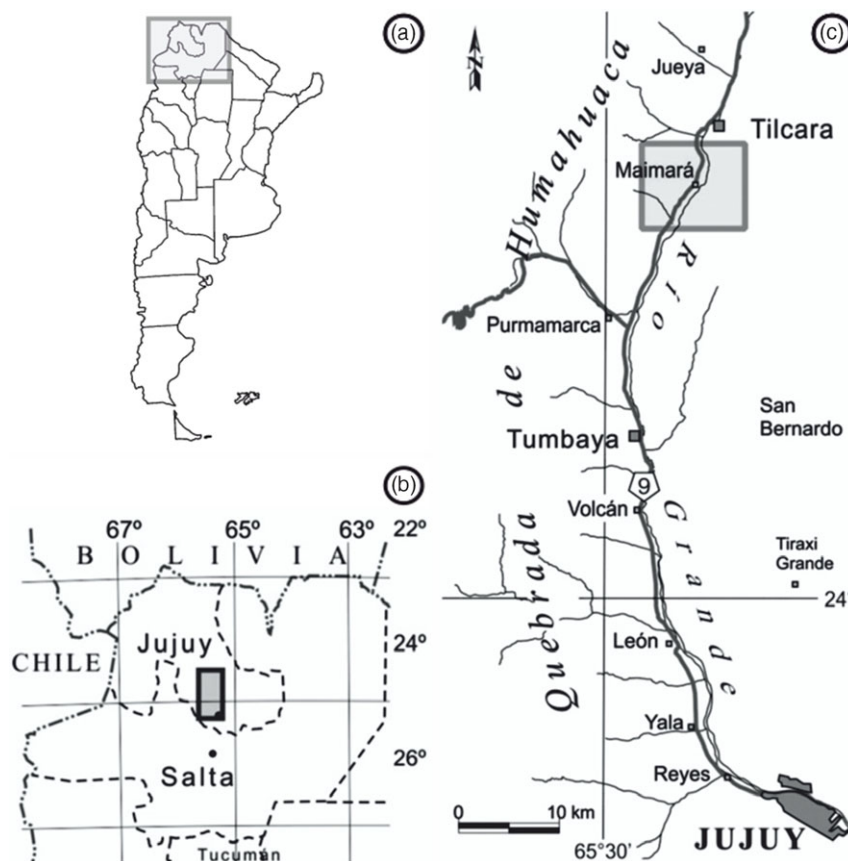


Fig. 1. Geographical location of the Maimará site. Modified from Cónsole-Gonella *et al.* (2017). (a) Political map of Argentina, South America. Grey rectangle indicates the location of (b). (b) Political map of northwestern Argentina. The grey rectangle indicates the location of (c). (c) Map of the Quebrada de Humahuaca, Jujuy province, displaying the location of the Maimará site (grey rectangle).

Cooper *et al.* (2013), Perissinotto *et al.* (2014), Suosaari *et al.* (2016b) and Edwards *et al.* (2017) were also considered.

High-resolution digital photogrammetry was used to obtain a reliable representation of the 3D stromatolite external morphology and architecture. A close-range photogrammetric survey was conducted, and 442 images were selected to achieve a good image overlap. Images were acquired using a 24-megapixel reflex digital camera with 27 mm focal length (43.2 mm equivalent) and pixel size $3.84 \times 3.84 \mu\text{m}$. A 3D textured mesh was generated by the software Agisoft Metashape Pro (version 1.5.2, Educational License). To correctly scale the model, a set of metric reference markers was used. The 3D model was converted to a false-colour topographic map using the software Paraview (version 5.4.1) (Figs. 5, 6b). The tidal reconstructions (see also online Supplementary Material S1 and S2, available at <http://journals.cambridge.org/geo>) were designed using the software Blender (version 2.81).

Internal morphology of stromatolites was described using polished slabs and thin-sections in the laboratory. The macrostructure and mesostructure were described using the classification proposed by Logan *et al.* (1964) and Horodyski (1977). We use the following abbreviations *sensu* Logan *et al.* (1964) in the text: SH-C – internal structure of hemispheroids vertically stacked with a constant basal radius; SH-V – internal structure of hemispheroids vertically stacked with a variable basal radius; and LLH-C – internal structure of closed laterally linked hemispheroids. In analysing microstructure, we focused on different parameters such as

lamination types, stacking patterns of laminae, lateral and vertical continuity of lamination, growth dynamics, hiatuses and/or disruptions in laminae, among others. Tidal channels were assessed and discussed adopting some concepts by Sarjeant (1975). Laminae were described based on their composition, lateral continuity, thicknesses and geometrical arrangement. Study of erosional structures was based on the criteria of Schneider (1977), Scholle (1978) and Cevallos-Ferriz & Werber (1980).

The percentage of porosity was estimated by point counting and its analysis was based on the classification proposed by Choquette & Pray (1970) and the descriptive and genetics concepts of Alonso *et al.* (1987) and Ahr *et al.* (2011). The description of the carbonates was carried out using the scheme proposed by Folk (1959) and Kendall *et al.* (2011).

4. Results

4.a. Overall depositional architecture and external morphology

The analysed level MNE5 ranges over 100–125 cm in thickness (Figs. 4b, 5a). MNE5 level is made up of stromatolitic domes with diameters ranging from 60 to 150 cm (Fig. 5a, b), forming a bioherm megastructure. The domes are distributed in three different groups according to their heights: the smallest (40–45 cm), a second group (45–55 cm), and the more developed (55–70 cm)

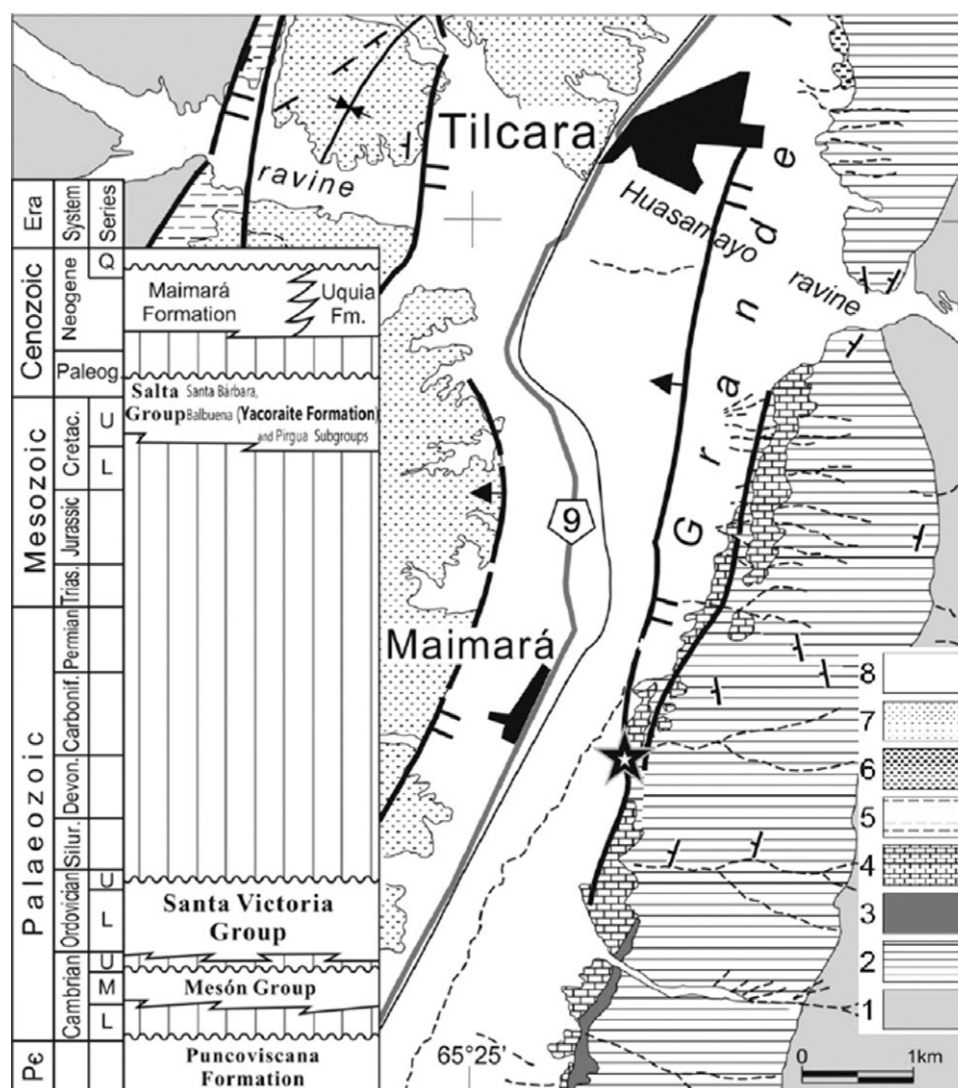


Fig. 2. Geological setting and stratigraphy of the study area. 1, Puncoviscana Formation (upper Precambrian–lower Cambrian); 2, Mesón Group (middle–upper Cambrian); 3, Ordovician?; 4, Balbuena Subgroup (Lecho and Yacoraite formations; Maastrichtian–Danian); 5, 6, Maimará and Uquia formations (Neogene); 7, 8, Quaternary. The star indicates the location of the Maimará section. After Cónsole-Gonella *et al.* (2017).

(Fig. 5c). All the stromatolites are on the top of the same palaeosurface of sedimentation (calcareous sandstone layer), where some depressions are observed (Fig. 5c).

Stromatolites occur as isolated domes or are organized in clusters of domes (Fig. 5a–c). The isolated domes are scarcer and smaller, with diameters ranging from 30 to 50 cm and heights less than 45 cm (Fig. 5c). The clusters are delimited by channels up to the lower middle tier surface (in green colours). Cluster exhibits up to five domes ranging from 40 to 65 cm in height, extending over areas up to 10 m². There are ten fully exposed clusters, although the other four clusters are partially covered by the overlying shale layers (Fig. 5c; online Supplementary Fig. S1a, available at <http://journals.cambridge.org/geo>).

The 3D elevation model shows that the middle tier cluster (in green colours) forms elongated structures with preferred orientation in the E–W direction, mainly ESE–WNW direction (Fig. 5c; online Supplementary Fig. S1a). Sometimes, these elongated structures can approach or even coalesce laterally along the length of the rows, producing compound masses with elongation normal to that of the primary elongation. In the top tier (in orange and reddish

colours), the clusters acquire more symmetrical domic shapes (Fig. 5c; online Supplementary Fig. S1a).

Both stromatolite clusters and individual domes are characterized by the occurrence of multiscale arrangement of channels (first, second and third order) (Fig. 6a). First-order channels refer to passages ranging from 30 to 100 cm in width and showing straight organization. As for the elongation of the middle tier clusters, these channels are aligned in the ESE–WNW direction (online Supplementary Fig. S1b). Second-order channels have an average of 20 cm width, separate domes within clusters and connect first-order channels to each other, adapting their morphology to the space between domes (Fig. 6b).

MNE5 stromatolites show a hemispheroidal external morphology (Fig. 7a), where the lateral development is greater than the vertical development (Fig. 7b, c). The external surface of the stromatolites is irregular, composed of small crests (diameters from 0.2 to 1 cm) and is lined with cavities filled with sediments. These cavities, referred to as third-order channels (Figs. 6a, 7d), give the domes a ‘cerebroid’ appearance (e.g. Pratt & James, 1982).



Fig. 3. (Colour online) Drone view of the working area. Stromatolites are indicated by a yellow star.

4.b. Internal morphology

Stromatolites exhibit a highly convex growth profile. The internal morphology is almost homogeneous, prevailing laminated columnar structures, which allows to describe an internal structure as a type columnar with branch (*sensu* Horodyski, 1977) (Fig. 8a). However, a basal sector (up to *c.* 3 cm in height) without a defined internal structure and the presence of isolated laminae is observed while, in the more developed domes, the top (in the last *c.* 3 cm) shows continuous lamination (Fig. 8a).

4.b.1. Mesostructure

The basal sector (up to *c.* 3 cm in height) is composed of uniform micrite, with the minor presence of well-developed, up to 1-mm-thick, laminae, isolated and interrupted throughout their lateral development (Fig. 8a, b). The rest of the dome exhibits an internal geometry of SH type, displaying laminated columns of both mode C and mode V. The SH-C structures are more common in the central and upper part of domes, while the SH-V are more common at the base and along flanks (Fig. 8a–c). Some columns are joined together at the top of domes (the last *c.* 3 cm) with a height greater than 55 cm, giving rise to the internal morphologies of LLH-C type (Fig. 8d).

Columns are developed with widths ranging from 0.3 to 2.5 cm. Some columns display upwards-developing branches with smaller-diameter (0.1 cm) columns. The laminae composing the columnar structures, up to 1 mm thick, are convex upwards and the edges of the columns are coalescent (Fig. 8c). Inside columns, random laminae with ferrous tonalities (Fig. 8c) and laminae with ooids (online Supplementary Fig. S2) can be observed (see Section 4.b.2).

The columns are separated from each other by third-order channels. These channels are cavities of variable width (0.1–0.8 cm) with irregular edges. The development plane of these cavities is perpendicular to the lamination. Third-order channels are filled with clastic material immersed in a micritic matrix, and are discussed in the following section (Fig. 8c).

4.b.2. Microstructure

Microstructure is characterized by the alternation of dark dense micritic laminae with lighter micritic to microsparitic laminae, giving rise to an alternating simple lamination (*sensu* Monty, 1976) (Fig. 9a, b). Dark laminae have an average thickness of 0.5 mm, and lighter laminae have an average thickness of 0.4 mm. Both dark dense micritic laminae and lighter micritic to microsparitic laminae present close texture, diffuse boundaries and transitional contacts (Fig. 9a, b). In some sectors there are a few sparitic laminae, up to 0.3 mm in thickness (which usually remains constant), with good lateral continuity, slight sinuosity and a fibrous texture (Fig. 9c).

Ferrous levels are also observed with a thickness of less than 0.1 mm, interrupted laterally and retracted (Fig. 9d). In addition to this, random laminae with clastic material also stand out (up to 1 mm in thickness) (Fig. 9e, f). They are composed of ooids (up to 0.4 mm diameter), semi-rounded micritic intraclasts (up to 0.2 mm diameter) and lithic fragments (up to 0.2 mm diameter) (Fig. 9e, f).

Throughout the microstructure, the lamination is interrupted by the third-order channels ranging from 1 to 8 mm in diameter (Fig. 10a). They have sinuous and irregular edges, and a direction of development perpendicular to the lamination plane. The lamination upon reaching this cavity curves downwards, overlapping

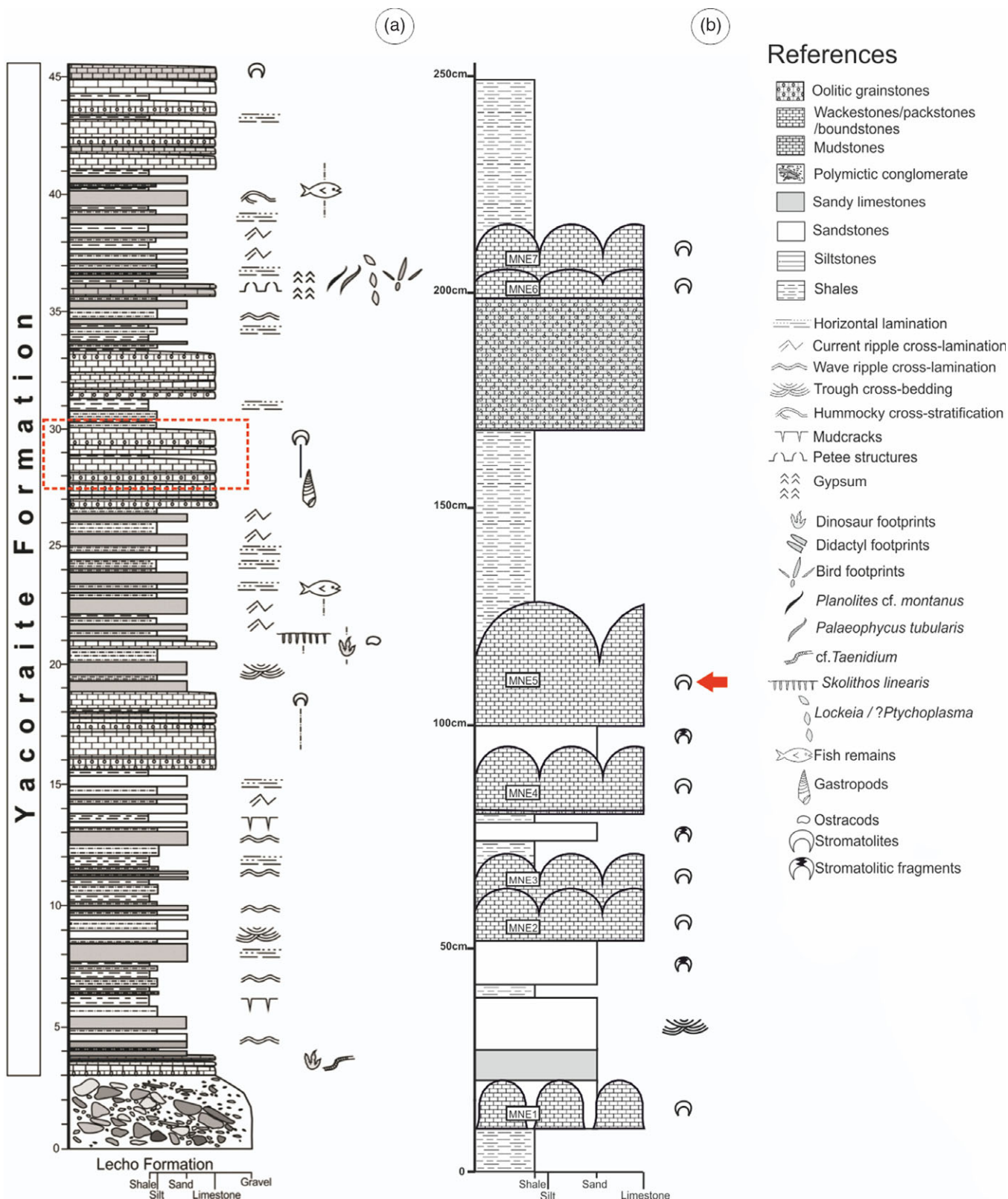


Fig. 4. (Colour online) Stratigraphic column of the outcrop. (a) Integrated logged section in Maimará. Modified from Cónsole-Gonella *et al.* (2017). (b) Detailed logged section. The red arrow indicates the stromatolite level MNE5.

each other (Fig. 10b). Third-order channels are filled with a micrite matrix with the main presence of ooids dispersed heterogeneously, semi-rounded micritic intraclasts (up to 1.5 mm diameter), quartz

grains (up to 0.2 mm diameter) and ostracods (up to 0.8 mm diameter) (Fig. 10c), forming a packed biomicrite texture. Ooids are spherical and elliptical with a concentric pattern, and are up to

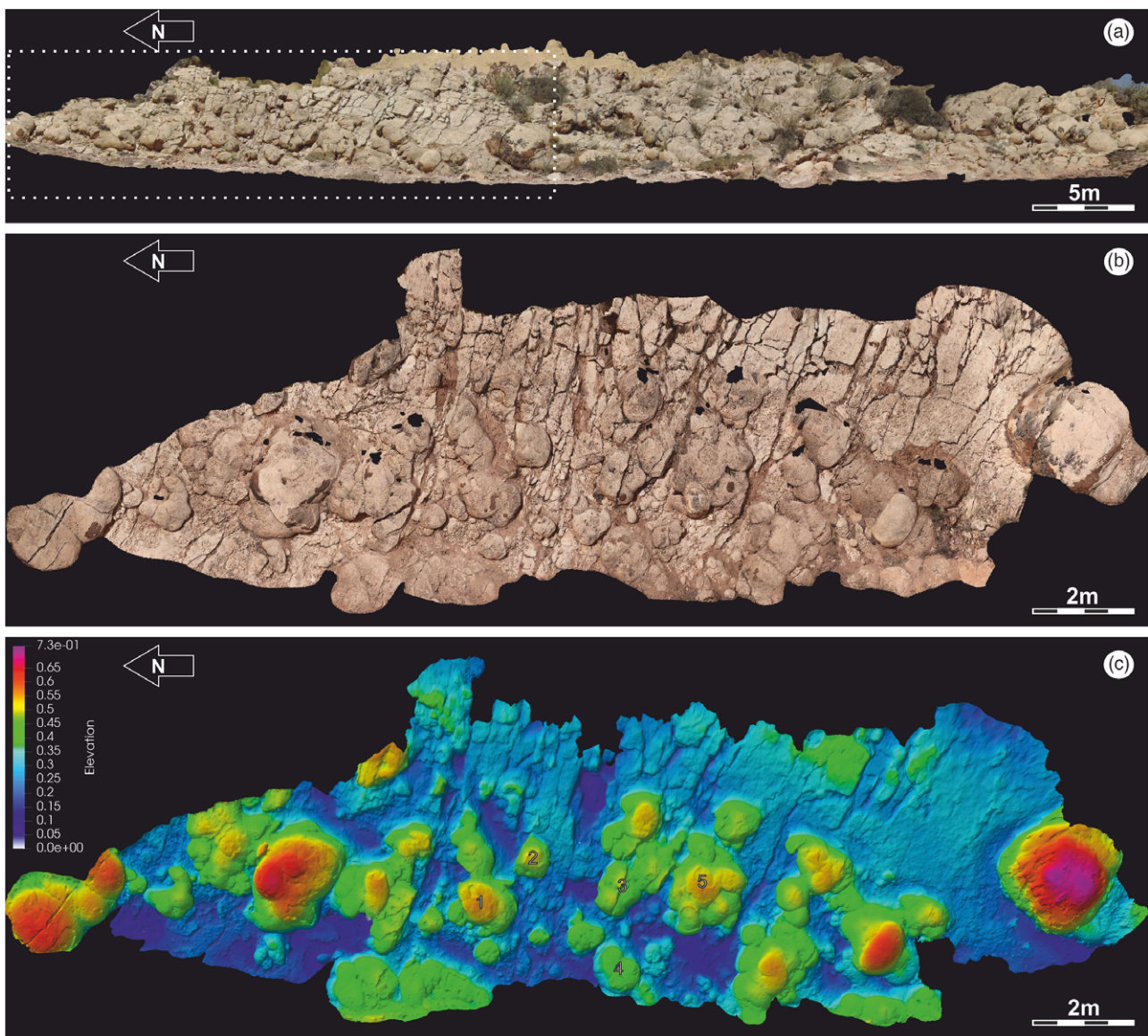


Fig. 5. (Colour online) 3D model of the outcrop obtained with digital photogrammetry. (a) Orthomosaic of the whole stromatolite outcrop. The white dotted area indicates the best preserved group of clusters. (b) Orthomosaic delimited within the highlighted area of (a). (c) Elevation model of (b). The figure shows ten fully exposed clusters, four partially covered clusters and more than ten individual domes. Palaeosurface of sedimentation is represented with blue colorimeters. The numbers indicate the position of the clusters and domes with respect to Fig. 6b.

2 mm in diameter. The nuclei are composed of carbonate or quartz fragments. Common aragonitic alteration is observed at the outer edges (Fig. 10d).

The estimated average porosity reaches a total of 36.20%. Two kinds of fenestral fabrics are observed: (1) irregular voids, horizontally elongate and parallel to bedding with a thickness of up to 0.25 mm (Fig. 10e) are the most abundant; and (2) bubble-like vugs, parallel to bedding with a thickness up to 0.3 mm. In addition to fenestral porosity, vacuolar, cavern and interparticle pore morphologies are also observed (Choquette & Pray, 1970) (Fig. 10f).

5. Discussion

Although the architecture of stromatolitic deposits can be conditioned by the microorganisms that produce them (van de Vijzel *et al.* 2020), the middle tier cluster and the first-order channels

show a preferred orientation that suggest the influence of unidirectional hydrodynamic energy in an intertidal environment (Hoffman, 1973, 1976a, b; Reid & Browne, 1991). Based on comparisons with modern analogues, elongated stromatolitic structures usually show preferred orientation parallel to water movement and with channels perpendicular to the coastline (Hoffman, 1973, 1976a, b; Reid & Browne, 1991).

Isolated stromatolites and the upper parts of the clusters present domical external morphology. In modern analogues, dome forms are interpreted as a response to minimize hydrodynamic energy (e.g. Gebelein, 1969; Dill *et al.* 1986; Andres & Reid, 2006; Suosaari *et al.* 2016b); however, these forms also occur in restricted and partially restricted environments, such as lagoons or lakes (e.g. Reitner *et al.* 1996; Cohen *et al.* 1997; Grey & Planavsky, 2009). Stromatolites studied here have similarities to those developing in environments of low hydrodynamic energy (e.g. Moore & Burne, 1994; Reitner

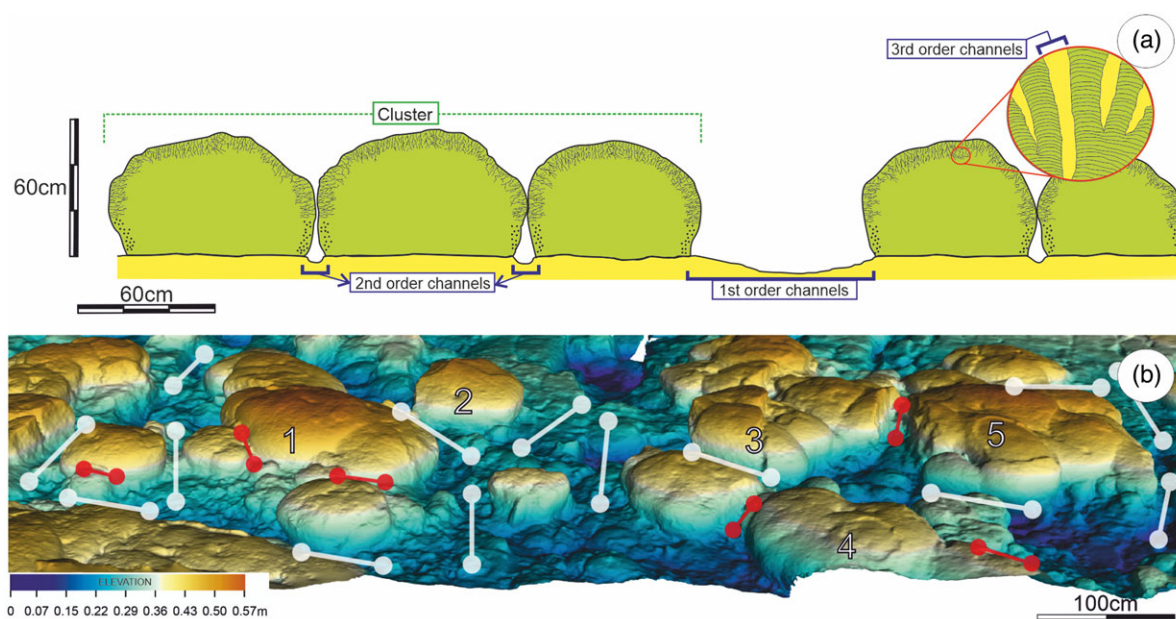


Fig. 6. (Colour online) Channel reconstruction. (a) Channel classification by order and relative dimensions at section view of clusters. (b) 3D photogrammetric elevation model of best preserved clusters. First-order channels are indicated with white lines, second-order channels with red lines. The numbers indicate the cluster position in Figure 5c.

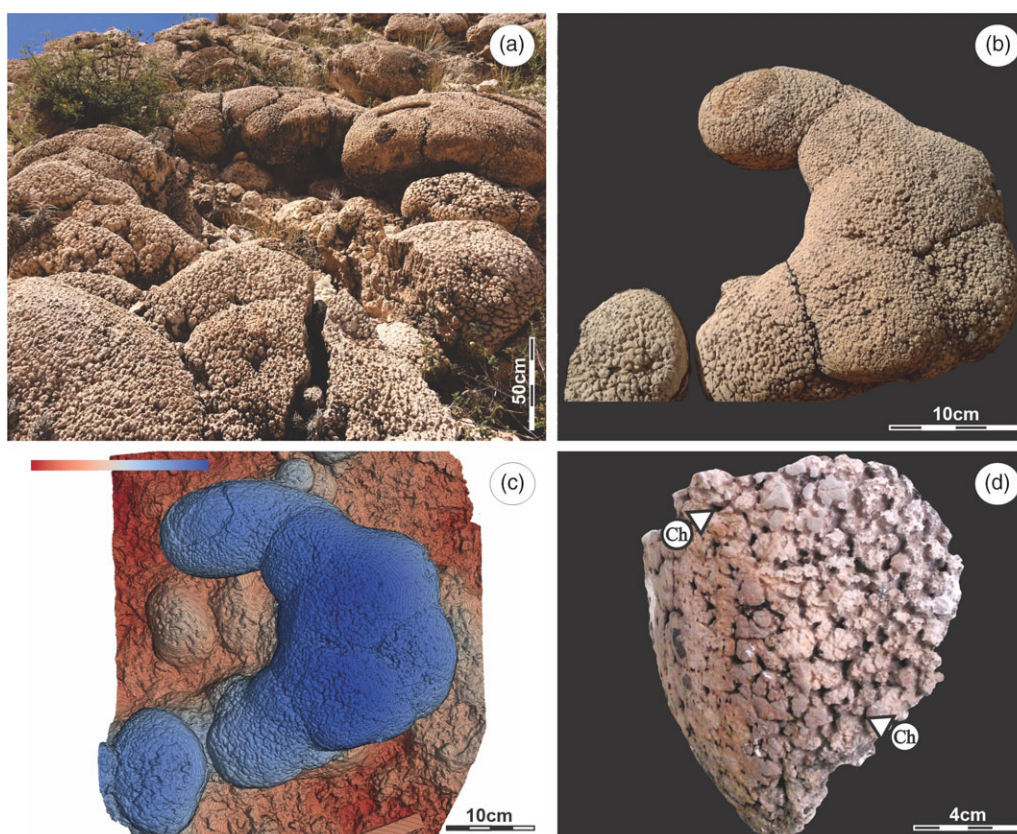


Fig. 7. (Colour online) External morphology and appearance. (a) Outcropping view of stromatolites. (b, c) Photography and 3D topography reconstruction of a cluster. The basal substratum and small domes are indicated by red, and well developed domes integrating the cluster are highlighted in blue. (d) Detailed view of the cerebroid surface appearance of a stromatolite dome. Cavities filled with sediments are called third-order channels (Ch).

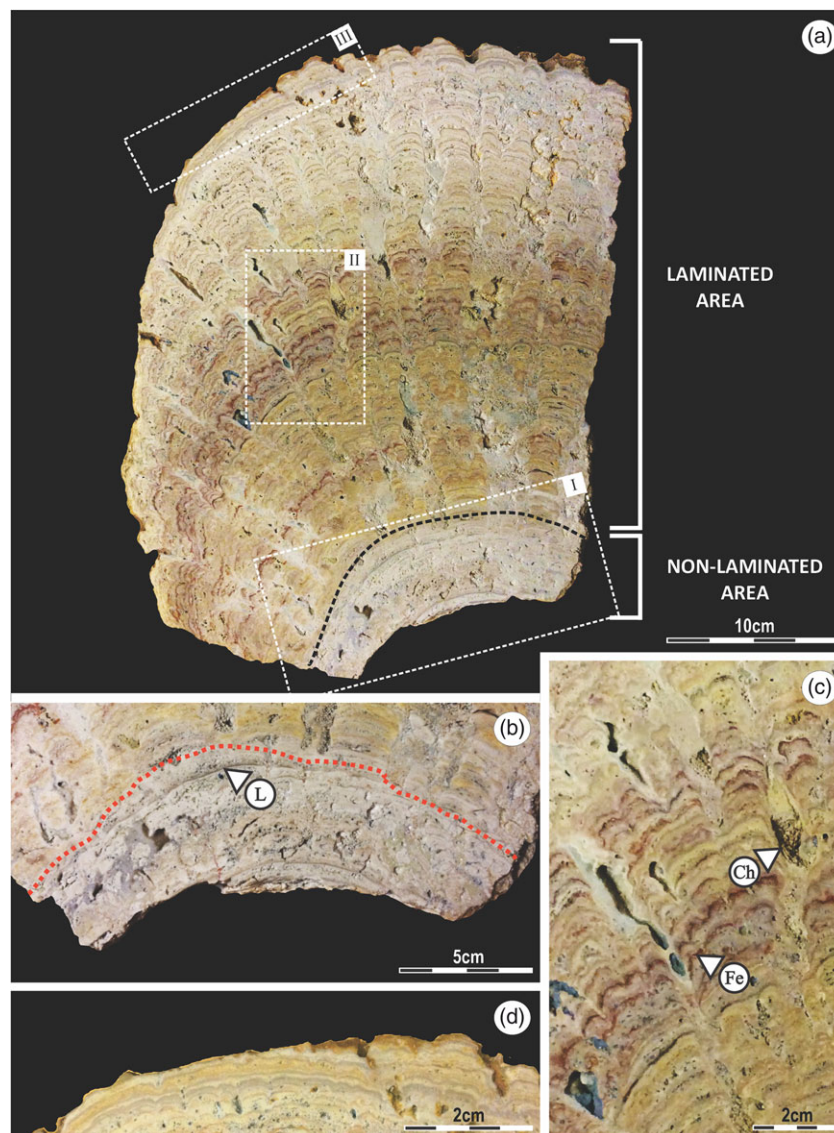


Fig. 8. (Colour online) Polished section (collection code: PIL 17.150, sample code: MNE5-P). (a) Two areas with different lamination patterns can be observed: there is a non-laminated area at the base, while from the middle to the top the structure is laminated. (b) Area I of the basal sector. Interrupted lamination (L) in a sparite matrix. (c) Area II of a SH mesostructure. Column structures are separated by third-order channels (Ch). Laminae with ferrous tonalities (Fe). (d) Area III of a LLH-C mesostructure.

et al. 1996; Grey & Planavsky, 2009; Wacey *et al.* 2018) regarding external morphology and simple branching columns. At the same time, different orders of magnitude in hydrodynamics suggest a partially restricted environment but not entirely indifferent to the action of the waves and tide (Eckman *et al.* 2008; Arenas & Pomar, 2010).

Accommodation space available for stromatolite growth and development is basically represented by water depth (vertical space) and substrate availability (lateral space). Vertical growth of domes is depth dependent (Kah *et al.* 2006; Bergman *et al.* 2010). As observed in current environments, different heights of domes present in the deposit indicate intervals of stability as the depth of the environment changes (e.g. Jahnert & Collins, 2012; Suosaari *et al.* 2016a). On the other hand, lateral development of stromatolites is controlled by substrate availability, which in turn is limited by the adjoining domes or by the channels of first and second order. Water run-off concentrates along these channels, preventing the lateral development of the stromatolites and

favouring domic morphologies due to their reduced resistance to hydrodynamic conditions (Gebelein, 1969).

The presence of depressions in the palaeosurface of sedimentation is probably related to erosive areas where the water swirls during the changing tides, where first-order channels connect (see Figs. 6c, 7b).

5.a. The influence of hydrodynamic conditions and factors in internal morphology

The internal structure is also a reflection of hydrodynamic conditions (Logan *et al.* 1964; Aitken, 1967; Hoffman, 1973; Acosta *et al.* 1988). The columnar structures are probably a response to reduce energy conditions (Dupraz *et al.* 2006), although we cannot rule out the influence of biotic factors (von der Borch *et al.* 1977).

Dupraz *et al.* (2006) suggested that the presence of columnar structures depends on a factor called 'attraction distance', which is a model of the attraction force of the build-up. An increase in

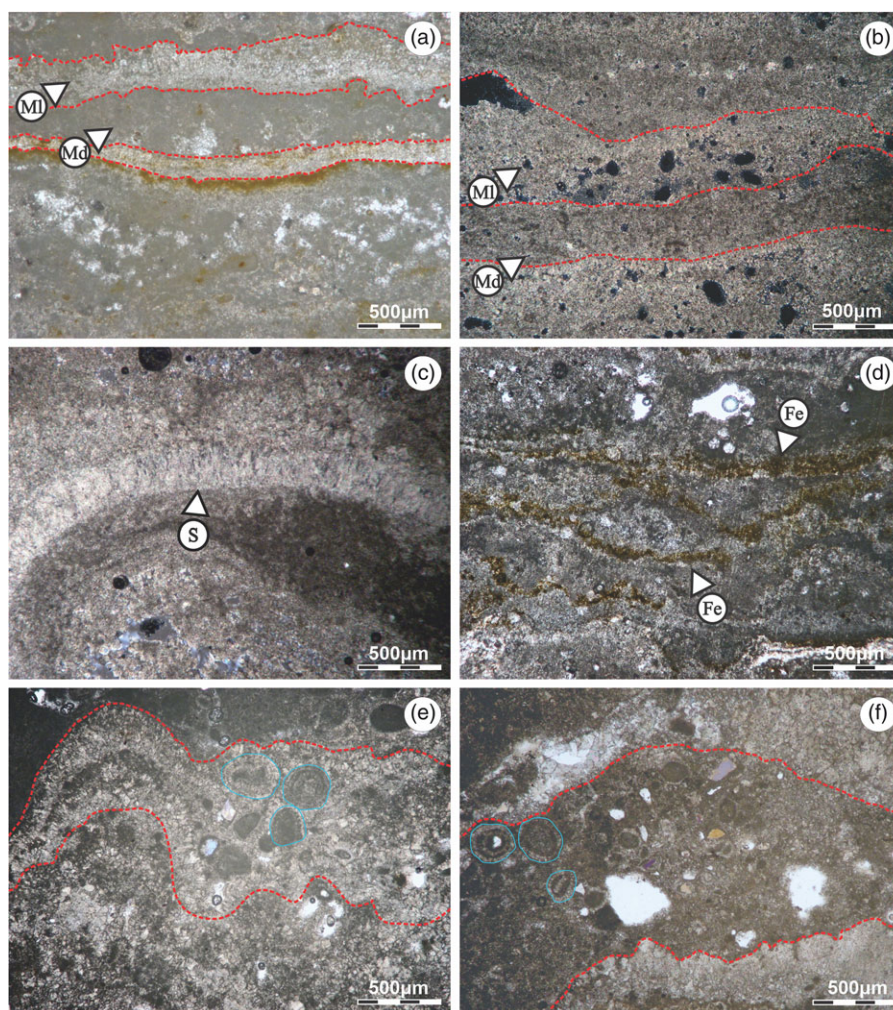


Fig. 9. (Colour online) Collection code: PIL 17.165. (a, b) Alternating dark dense micritic laminae (Md) with lighter micritic (Ml) to microsparitic laminae. The laminae are poor in intraclasts, with close texture, diffuse boundaries and transitional contact. (c, d) Thin-section MNE5-T1: (c) isolated lamina of sparitic composition (S) with slight sinuosity and fibrous texture; (d) ferrous levels (Fe) with a thickness of < 0.1 mm, interrupted laterally and retracted. (e, f) Thin-section MNE5-T5: laminae with clastic material composed of ooids (light blue circles), semi-rounded micritic intraclasts and lithic fragments.

the attraction distance leads to larger protection zones where no growth is possible and produces the formation of wider-spaced columnar or branching morphologies. The protection zones can be the result of differential erosive effects during water run-off through small escape routes (i.e. third-order channels), truncating the *in vivo* microbial mats growth (Schneider, 1977; Cevallos-Ferriz & Werber, 1980; Shapiro & Awramik, 2000). However, columnar structures can be found in stromatolites from restricted and partially restricted environments, where the filling of the third-order channel (ooids, micritic intraclasts and ostracods) confirm the influence of tides and waves in its development (Altermann, 2008).

Branching of the stromatolite columns may be due to changes in the sediment supply and/or a change in the composition of the microbial community (Planavsky & Grey, 2008; Mackey *et al.* 2015). Although it is not possible to know precisely which of these two processes was predominant, branching appears to be closely related to a decrease in sediment supply, the product of an increase in depth that would have decreased hydrodynamic energy, resulting in more stable environmental conditions in which the microbially mediated framework growth began to control stromatolite

morphology (Planavsky & Grey, 2008; Mackey *et al.* 2015). The width of the columns was controlled by the accommodation space inside the stromatolite, which was limited by the third-order channels and domical morphology (Horodyski, 1977).

The LLH-C structures located in the upper area of stromatolites can be explained as a reduction in the hydrodynamic energy of the system with respect to SH structures (Logan *et al.* 1964; Dupraz *et al.* 2006). This energy reduction allows microbial mats to colonize the entire surface of the stromatolite, giving rise to a continuous laminar structure.

Laminated micrite/microsparite is interpreted as a primary depositional microstructure (Reid *et al.* 2003). The predominance of this microstructure and the low content of clastic material in the lamination suggest that growth of stromatolites was controlled by the *in situ* precipitation of carbonate with the influence of microbial activity (Reid *et al.* 2000). Alternation between micritic and microsparitic laminae is attributed to a variation in the predominance of nucleation and crystallization processes during the growth of the stromatolite (Riding, 2000; Dupraz *et al.* 2009). This can be produced by different factors, such as the hydrodynamic energy, changes in the precipitation rate, changes in

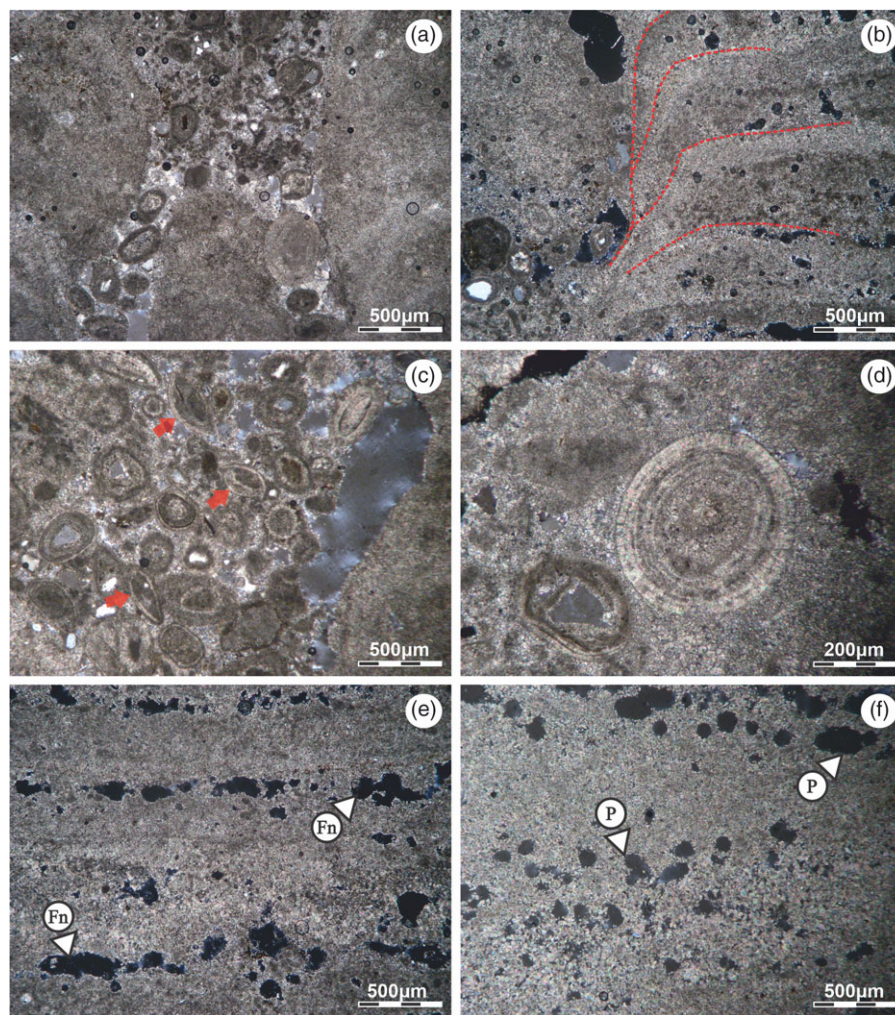


Fig. 10. (Colour online) Collection code: PIL 17.165. (a, b) Thin-section MNE5-T2: (a) Cavities (third-order channels) interrupting the lamination. (b) Edges of the channels with an orientation of development perpendicular to the lamination plane. The lamination (red lines) deflects downward reaching the cavity. (c, d) Thin-section MNE5-T3: (c) third-order channels filled with oo-micritic material; Ostracods are indicated with red arrows; (d) Spherical ooid with detrital nuclei and concentric shape. (e, f) Thin-section MNE5-T4: (e) fenestral porosity (Fn): consists of irregular voids, horizontally elongate, and parallel to bedding with a thickness up to 0.25 mm; (f) vacuolar porosity (P) (non-selective factory).

saturation, level of organic activity, and/or fluctuation of carbonate and calcium concentration (Giuffrè *et al.* 2013; Dobberschütz *et al.* 2018; Li & Jun, 2019).

Although the stromatolites studied in this manuscript cannot be classified as ‘agglutinated stromatolites’ (*sensu* Riding *et al.* 1991), laminae with clastic material (including ooids) developed when carbonate sand was remobilized by water currents and grains were trapped within the microbial mats. This suggests a pause in *in situ* precipitation of carbonate and a momentary predominance of trapping and binding (Suárez-González *et al.* 2014, 2016).

Conditions for ooid trapping by stromatolites may be preferentially achieved in tidally influenced environments, under shallow to very shallow water conditions. Constant grain availability in the environment is necessary to trap ooids and other carbonate particles, which is common in intertidal environments where grains were mobilized by tides in addition to waves and episodic storms (Suárez-González *et al.* 2016).

In the MNE5 stromatolites of Maimará, laminae with clastic material appear to be limited by two factors: (1) a decrease in sediment supply, the product of an increase in water level (Altermann, 2008); and (2) the size of the clasts (as observed in the channels)

exceeding the thickness of the lamination, which complicates their capture (Riding *et al.* 1991; Altermann, 2008).

Fenestral porosity has a depositional genesis product of two factors that can act separately or in combination: (1) retraction of the lamination, product of the desiccation; or (2) gas bubbles as a result of the decay of organic matter (Alonso *et al.* 1987; Mazzullo, 2004; Sanz-Montero *et al.* 2005). Several authors have suggested that fenestral porosity should be considered with certainty as indicative of upper intertidal to supratidal environments (Shinn, 1968, 1983; Chatalov, 2009; Mata *et al.* 2012). Vughs, caverns and interparticle pores have a genesis influenced by dissolution during diagenesis (Ahr *et al.* 2011).

5.b. Interpretation of channels

Based on comparisons with modern and fossil analogues, channels are interpreted as the result of the differential modelling and erosive effect during the run-off of water by tides and waves, preventing the lateral continuity of the stromatolite (e.g. Hoffman, 1976a; Schneider, 1977; Cevallos-Ferrix & Werber, 1980; Acosta *et al.* 1988; Andres & Reid, 2006; Jahnert & Collins, 2012).

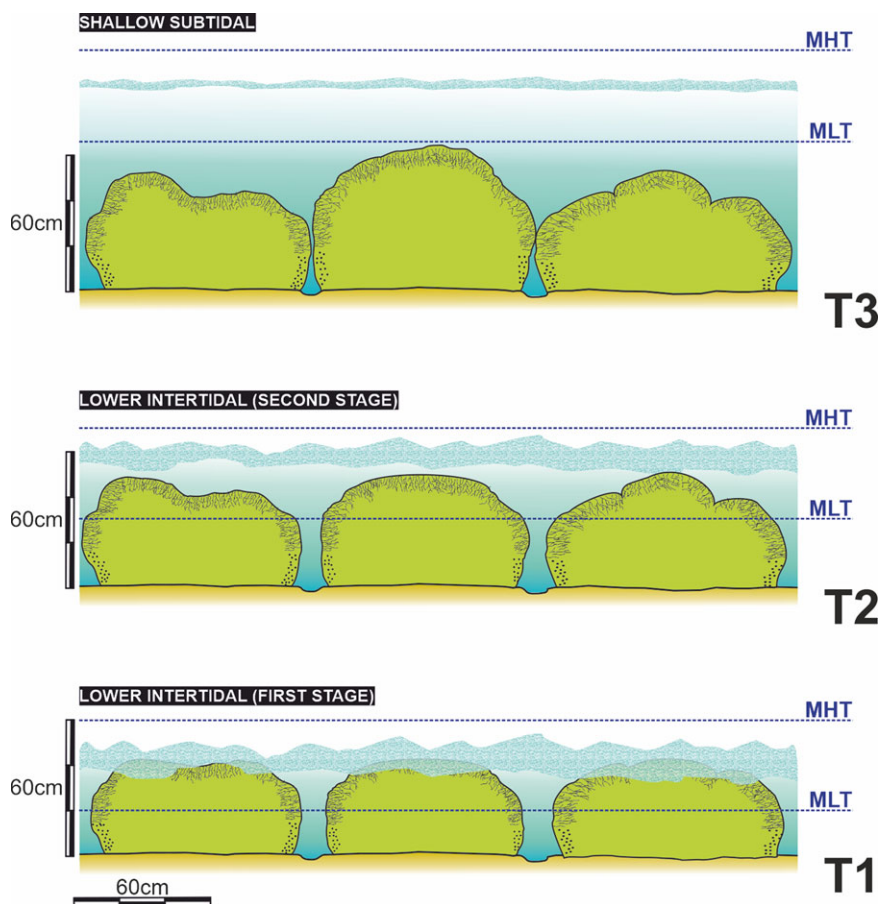


Fig. 11. (Colour online) Palaeoenvironmental evolution model of the stromatolites system. Depth conditions changed from lower intertidal (T1) to shallow subtidal (T3). T – time; MHT – mean high tide; MLT – mean low tide.

First-order channels (Figs. 5c, 6; online Supplementary Fig. 1b) represent areas with enhanced hydraulic stress (Cevallos-Ferriz & Werber, 1980). As seen in analogous deposits, they tend to develop perpendicular to the coastline (i.e. parallel to the hydrodynamic direction) with a clear hydraulic tendency (Hoffman, 1976b; Reid & Browne, 1991), suggesting that the tidal water and/or stream water transported through them achieved high hydrodynamic energy and prevented microbial development (Hoffman, 1976a; Andres & Reid, 2006). These channels would also concentrate rip currents, acting along with the hydrodynamic energy in two directions, making it difficult to locate and orient the coastline.

On the other hand, second-order channels were formed in areas with lower hydraulic energy after the run-off, which limited the lateral development of stromatolite structures (Figs. 5c, 6).

Third-order channels are spaces where the passage of water truncates the microbial mats *in vivo* (see Schneider, 1977; Cevallos-Ferriz & Werber, 1980; Shapiro & Awramik, 2000) (Figs. 6a, 8c, 10a, b). As observed in extant analogues influenced by waves and tides (e.g. Gebelein, 1969; Altermann *et al.* 2006), hydrodynamic energy acting along these channels prevents the formation of microbial mats, determining the development of a wedged and downwards-curved lamination.

Evidence indicating high-energy conditions is provided by the type of filling in the third-order channels, which occurs passively during the stromatolitic growth through the deposition of ooids. Concentric ooids with different nuclei and sizes, aragonitic

alteration at the edges and heterogeneously distributed in the channels, suggest good agitation and transport through different energy pulses (Rohrlich, 1974; Scholle, 1978; Frakes & Bolton, 1984).

Ostracods suggest partially restricted coastal areas, such as a lagoon (Palma, 1993; Carignano & Ballent, 2009). No evidence of bioturbation is observed in channel deposits or on their edges, and ostracods were not found in burrowing and grazing positions that suggest interaction with the stromatolites, so they are only considered para-autochthonous bioclasts.

5.c. Palaeoenvironmental model

The obtained results and the comparison with modern analogues allow to infer that the stromatolites from Maimará were developed in a lower intertidal to shallow subtidal environment close to the coastline (e.g. Hoffman, 1976a; Reid & Browne, 1991; Dupraz *et al.* 2006; Jahnert & Collins, 2012; Suosaari *et al.* 2016b). Indeed, outcrop architecture, clusters and channels distribution are quite similar to modern intertidal stromatolites of Shark Bay (Australia) (Hoffman, 1973, 1976b) and Stocking Island (Exuma Cays, Bahamas) (Reid & Browne, 1991), and middle Precambrian intertidal stromatolites (Canadian Shield) (Hoffman, 1976a), in which main orientation is perpendicular to the shore and parallel to palaeocurrents, similar to our study case. This interpretation agrees with and reinforces the previous palaeoenvironmental proposal of Cónsole-Gonella *et al.* (2017, 2021).

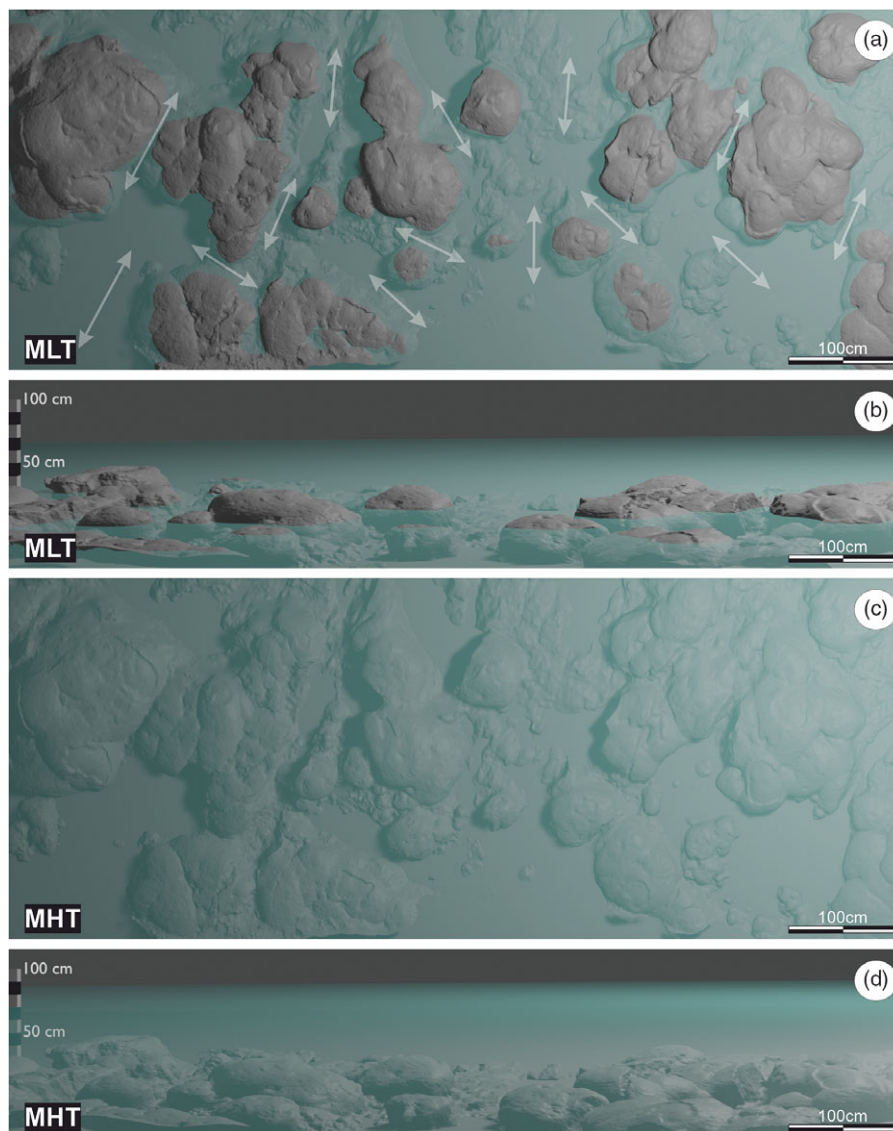


Fig. 12. (Colour online) 3D outcrop computer model representing the lower intertidal stage (T2 in Fig. 10). (a) Plan view during mean low tide (MLT). Note water run-off (arrows) along first- and second-order channels. (b) Side view during mean low tide. (c) Plan view during mean high tide (MHT). (d) Side view during mean high tide.

Some authors suggested the presence of stromatolites in lake systems in the southern sector of the basin (Metán–Alemania sub-basin) (Bunevich *et al.* 2017; Gomes *et al.* 2019; Deschamps *et al.* 2020). Given the size of the basin and its distance from Maimará locality (Tres Cruces sub-basin), it is accepted that this may be correct. However, tidal influence during deposition of the Yacoraite Formation in the southern sector of the Metán sub-basin (Cabra Corral locality, Salta province) was assessed by Marquillas *et al.* (2003, 2005) for the entire basin. In addition, stromatolite tidal deposits of the Yacoraite Formation were also recognized in Cabra Corral area by Hamon *et al.* (2012) and Cónsole-Gonella & Marquillas (2014). These authors described several stromatolite architectures related to restricted lagoon to tidal flat deposits (Hamon *et al.* 2012), consistent with the environmental setting proposed in our study section by Cónsole-Gonella *et al.* (2017).

The different heights reached by the domes are likely due to changes in water level, which controlled the upper limit of accommodation space (Kah *et al.* 2006; Arenas & Pomar, 2010; Bergman

et al. 2010). This information suggests an overall variation of water depth from 45 to > 70 cm, as observed in similar settings (e.g. Coorong Lagoon area in von der Borch, 1974).

In such a changing environment (from lower intertidal to shallow subtidal), it is difficult to determine which hydrodynamic factor played a dominant role (i.e. waves or tides). In a first stage, the stromatolites developed in a lower intertidal environment in which water depth was progressively increasing (second stage) (Fig. 11). The preferred orientation of the middle tier cluster and first-order channels, the presence of ferrous laminae in the lower and middle zone of the domes, the filling of the third-order channels and the internal structure of the SH type all suggest an environment with the hydrodynamic energy controlled by both waves and run-off of the water during the low tide (Logan *et al.* 1964; Hoffman, 1976a; Reid & Browne, 1991) (Figs. 12, 13; online Supplementary Fig. S2 and Supplementary Material S1).

As it is interpreted in modern analogues (Logan *et al.* 1964; Andres & Reid, 2006; Dupraz *et al.* 2006), transition from a SH structure to a LLH-C in the internal variation of the more



Fig. 13. (Colour online) Palaeoenvironmental reconstruction. Sunrise at Maimará lagoon. Note shorebirds at the left side. Artwork by Ignacio Díaz-Martínez and Carlos Cónsole-Gonella.

developed domes (Fig. 8c, d) indicates a decrease in hydrodynamic energy, probably as a result of an increase in water depth. The environment changed from lower intertidal to shallow subtidal (Fig. 11). This interpretation is indirectly sustained by the increased branching of the columns before the change to a LLH structure and the lack of desiccation cracks in the LLH structure (Kah *et al.* 2006; Planavsky & Grey, 2008; Mackey *et al.* 2015). As the depth increased, the waves lost prominence and sediment transport decreased (Bergman *et al.* 2010).

It is possible that tide predominated over waves during this stage, and was responsible for continuing to fill the third-order channels. However, it is difficult to determine their participation in the architecture of this outcrop because we cannot rule out a biological stabilization of the domes and clusters previously formed under intertidal conditions (van de Vijssel *et al.* 2020). This increase in water level must have taken place under stable conditions, without changes in the balance between physical, chemical and biological factors, because there are no signs of interruptions along dome growth.

6. Conclusions

A sedimentological and facies multi-scale analysis of three-dimensionally preserved stromatolites allowed us to understand variations in hydrodynamics and overall palaeoenvironment of the Yacoraite Formation at Maimará locality, highlighting a direct relationship with the morphostructural development of stromatolites. These stromatolites were developed in a palaeoenvironment that varied from lower intertidal (*c.* 40 cm deep) to shallow subtidal (> 70 cm deep), close to the coastline, partially restricted and affected by hydrodynamic action.

The architecture of the deposit was directly affected by the hydrodynamic energy of the palaeoenvironment. Clusters are limited by first-order channels, usually developed perpendicular to the coastline with a clear hydraulic tendency, suggesting the transport of tidal water and/or stream water through them. On the other hand, water dissipation after run-off limited the lateral development of stromatolites with the formation of second-order channels inside clusters. Hydrodynamic energy also influenced the internal

structure of the stromatolites. The structure of the SH type is explained as a product of hydrodynamic energy, where the third-order channels can be the result of differential erosive effects during run-off of water truncating the microbial mats *in vivo*. The increase in branching of the columns, and the subsequent transition from a SH structure to a LLH-C structure in the upper part of the domes of greater height, suggest an increase in water depth and a decay in the hydrodynamic energy of the palaeoenvironment where the waves lost prominence.

This new approach can also be applied in other subjects such as geochemistry and/or isotopic studies. Although our interpretation focuses on a specific area of the basin, it may be useful to evaluate similar records along the Late Cretaceous Central Andean basin.

Acknowledgements. This research was supported by grant PICT 2017-2057 (C. Cónsole-Gonella and S. de Valais) from the Agencia Nacional de Promoción Científica y Técnica (Argentina). We are grateful to the Maimará community and to colleagues R. Marquillas (Universidad de Salta and CONICET), M.C. Sánchez (Universidad Nacional de Salta), M. Griffin (Universidad Nacional de La Plata and CONICET) and P. Herrera-Oviedo (Universidad Nacional de Jujuy and CONICET) for their help in different stages of the fieldwork. We also thank Dr. Bas Van de Schootbrugge and two anonymous reviewers for their valuable comments on the manuscript.

Conflict of interest. None.

Supplementary material. To view supplementary material for this article, please visit <https://doi.org/10.1017/S0016756821000315>

References

- Acosta P, García Hernández M & Checa A (1988) Biohermos de esponjas y estromatolitos en la secuencia transgresiva oxfordiense de la Sierra de Cazorla. *Geogaceta* 5, 36–39.
- Ahr WM, Mancini EA and Parcell WC (2011) Pore characteristics in microbial carbonate reservoirs. *AAPG Search and Discovery Article* 30167, 10–13.
- Aitken JD (1967) Classification and environmental significance of cryptalgal limestones and dolomites, with illustrations from the Cambrian and Ordovician of southwestern Alberta. *Journal of Sedimentary Petrology* 37, 1163–78.

- Allwood AC, Walter MR, Kamber BS, Marsahl CP and Burch IW (2006) Stromatolite reef from the Early Archaean era of Australia. *Nature* **441**, 714–8.
- Alonso FJ, Ebert RM and Ordaz J (1987) Caracterización del sistema poroso de calizas y dolomías. *Boletín Geológico y Minero* **98**, 226–37.
- Altermann W (2008) Accretion, trapping and binding of sediment in Archean stromatolites-morphological expression of the antiquity of life. *Space Science Reviews* **135**, 55–79.
- Altermann W, Kazmierczak J, Oren A and Wright DT (2006) Cyanobacterial calcification and its rock-building potential during 3.5 billion years of Earth history. *Geobiology* **4**, 147–66.
- Andres MS and Reid RP (2006) Growth morphologies of modern marine stromatolites: a case study from Highborne Cay, Bahamas. *Sedimentary Geology* **185**, 319–32.
- Arenas C and Pomar L (2010) Microbial deposits in upper Miocene carbonates, Mallorca, Spain. *Palaeogeography, Palaeoclimatology, Palaeoecology* **297**, 465–85.
- Bergman KL, Westphal H, Janson X, Poiriez A and Eberli GP (2010) Controlling parameters on facies geometries of the Bahamas, an isolated carbonate platform environment. In *Carbonate Depositional Systems: Assessing Dimensions and Controlling Parameters* (eds H Westphal, B Riegl and GP Eberli), pp. 5–80. Dordrecht: Springer.
- Brackebusch L (1883) Estudios sobre la Formación Petrolífera de Jujuy. *Boletín de la Academia Nacional de Ciencias de Córdoba* **5**, 1–50.
- Bunevich RB, Borghi L, Gabaglia GP, Terra GJ, Freire EB, Lykawka R and Frago DG (2017) Microbialitos da Sequência Balbuena IV (Daniano), Bacia de Salta, Argentina: caracterização de intrabioarquitetas e de microciclos. *Pesquisas em Geociências* **44**, 177–202.
- Carignano AP and Ballent S (2009) Microfósiles (Foraminifera, Ostracoda) y su respuesta a las variaciones paleoambientales. Un ejemplo en la Formación Allen (Cretácico Superior), cuenca Neuquina, Argentina. *Ameghiniana* **46**, 307–20.
- Cevallos-Ferriz S and Werber R (1980) Arquitectura, estructura y ambiente de depósito de algunos estromatolitos del Precámbrico sedimentario de Caborca, Sonora. *Revista Mexicana de Ciencias Geológicas* **4**, 97–103.
- Chatalov A (2009) Primary and secondary fenestral porosity in Middle Triassic subtidal grainstones from the Belogradchik strip, NW Bulgaria: implications for unconformity-related diagenesis. *Comptes rendus de l'Académie bulgare des Sciences* **62**, 85–96.
- Choquette PW and Pray LC (1970) Geologic nomenclature and classification of porosity in sedimentary carbonates. *American Association of Petroleum Geologists Bulletin* **54**, 207–50.
- Clarke EC and Teichert C (1946) Algal structures in a Western Australian salt lake. *American Journal of Science* **224**, 271–6.
- Cohen AS, Talbot MR, Awramik SM, Dettman DL and Abell P (1997) Lake level and paleoenvironmental history of Lake Tanganyika, Africa, as inferred from late Holocene and modern stromatolites. *Geological Society of America Bulletin* **109**, 444–60.
- Cónsole-Gonella C, de Valais S, Sánchez MC and Marquillas R (2012) Nuevo registro de huellas de vertebrados en la Formación Yacoraite (Maastrichtiano-Daniano), Maimará, Cordillera Oriental argentina. *Ameghiniana* **49**, R141.
- Cónsole-Gonella C, de Valais S, Marquillas RA and Sánchez MC (2017) The Maastrichtian–Danian Maimará tracksite (Yacoraite Formation, Salta Group), Quebrada de Humahuaca, Argentina: environments and ichnofacies implications. *Palaeogeography, Palaeoclimatology, Palaeoecology* **468**, 327–50.
- Cónsole-Gonella C, Díaz-Martínez I, Cíttón P and de Valais S (2021) New record of Late Cretaceous vertebrate tracks from the Yacoraite Formation (Juella, Quebrada de Humahuaca, northwestern Argentina): aerial drone survey, preservation and sedimentary context. *Journal of South American Earth Sciences* **107**, 103116, <https://doi.org/10.1016/j.jsames.2020.103116>.
- Cónsole-Gonella C and Marquillas RA (2014) Bioclastration trace fossils in epeiric shallow marine stromatolites: the Cretaceous–Paleogene Yacoraite Formation, Northwestern Argentina. *Lethaia* **47**, 107–19.
- Cooper JAG, Smith AM and Arnscheidt J (2013) Contemporary stromatolite formation in high intertidal rock pools, Giant's Causeway, Northern Ireland: preliminary observations. *Journal of Coastal Research* **65**, 1675–80.
- Cumings ER (1932) Reefs or bioherms? *Bulletin of the Geological Society of America* **43**, 331–52.
- d'Orbigny A (1842) Voyage dans l'Amérique méridionale. *Paléontologie* **10**, 188.
- Davaud E, Strasser A and Jedoui Y (1994) Stromatolite and serpulid bioherms in a Holocene restricted lagoon (Sabkha El Melah, southeastern Tunisia). *Phanerozoic Stromatolites* **2**, 131–51.
- Deschamps R, Rohais S, Hamon Y and Gasparrini M (2020) Dynamic of a lacustrine sedimentary system during late rifting at the Cretaceous–Palaeocene transition: Example of the Yacoraite Formation, Salta Basin, Argentina. *The Depositional Record* **6**, 490–523.
- Díaz-Martínez I, de Valais S and Cónsole-Gonella C (2016) First evidence of *Hadrosauropodus* in Gondwana (Yacoraite Formation, Maastrichtian–Danian), northwestern Argentina. *Journal of African Earth Sciences* **122**, 79–87.
- Dill RF, Shinn EA, Jones AT, Kelly K and Steinen RP (1986) Giant subtidal stromatolites forming in normal salinity waters. *Nature* **324**, 55–58.
- Dobberschütz S, Nielsen MR, Sand KK, Civioci R, Bovet N, Stipp SLS and Andersson MP (2018) The mechanisms of crystal growth inhibition by organic and inorganic inhibitors. *Nature Communications* **9**, 1–6.
- Dupraz C, Pattisina R and Verrecchia EP (2006) Translation of energy into morphology: simulation of stromatolite morphospace using a stochastic model. *Sedimentary Geology* **185**, 185–203.
- Dupraz C, Reid RP, Braissant O, Decho AW, Norman RS and Visscher PT (2009) Processes of carbonate precipitation in modern microbial mats. *Earth-Science Reviews* **96**, 141–62.
- Eckman JE, Andres MS, Marinelli RL, Bowlin E, Reid RP, Aspden RJ and Paterson DM (2008) Wave and sediment dynamics along a shallow subtidal sandy beach inhabited by modern stromatolites. *Geobiology* **6**, 21–32.
- Edwards MJK, Anderson CR, Perissinotto R and Rishworth GM (2017) Macro- and meso-fabric structures of peritidal tufa stromatolites along the Eastern Cape coast of South Africa. *Sedimentary Geology* **359**, 62–75.
- Folk RL (1959) Practical petrographic classification of limestones. *AAPG Bulletin* **43**, 1–38.
- Forbes M, Vogwill R and Onton K (2010) A characterisation of the coastal tufa deposits of south-west Western Australia. *Sedimentary Geology* **232**, 52–65.
- Frakes LA and Bolton BR (1984) Origin of manganese giants: sea-level change and anoxic-oxic history. *Geology* **12**, 83–86.
- Gebelein CD (1969) Distribution, morphology, and accretion rate of recent subtidal algal stromatolites, Bermuda. *Journal of Sedimentary Petrology* **39**, 49–69.
- Gebelein CD (1976) Open marine subtidal and intertidal stromatolites (Florida, The Bahamas and Bermuda). In *Stromatolites* (ed WR Walter), pp. 20, 381–8. Amsterdam: Elsevier.
- Giuffrè AJ, Hamm LM, Han N, De Yoreo JJ and Dove PM (2013) Polysaccharide chemistry regulates kinetics of calcite nucleation through competition of interfacial energies. *Proceedings of the National Academy of Sciences* **110**, 9261–6.
- Golubic S (1976) Organisms that build stromatolites. In *Stromatolites* (ed WR Walter), pp. 20, 113–26. Amsterdam: Elsevier.
- Gomes JPB, Bunevich RB, Tonietto SN, Alves DB, Santos JF and Whitaker FF (2019) Climatic signals in lacustrine deposits of the Upper Yacoraite Formation, Western Argentina: evidence from clay minerals, analcime, dolomite and fibrous calcite. *Sedimentology* **67**, 2282–309.
- Grey K and Planavsky NJ (2009) Microbialites of Lake Thetis, Cervantes, Western Australia: a field guide. Geological Survey of Western Australia, Government of Western Australia, *Record* 21 p.
- Grotzinger JP and Knoll AH (1999) Stromatolites in Precambrian carbonates: evolutionary mileposts or environmental dipsticks? *Annual Review of Earth and Planetary Sciences* **27**, 313–58.
- Hamon Y, Rohais S, Deschamps R and Gasparrini M (2012) Outcrop analogue of pre-salt microbial series from South Atlantic: the Yacoraite Fm, Salta rift system (NW Argentina). In *Proceedings of the AAPG Hedberg Conference "Microbial Carbonate Reservoir Characterization"*, 4–8 June 2012, Houston.
- Hoffman P (1973) Recent and ancient algal stromatolites: seventy years of pedagogic cross-pollination. In *Evolving Concepts in Sedimentology* (ed. RN Ginsburg), pp. 178–91. Baltimore: John Hopkins University Press.
- Hoffman P (1976a) Environmental diversity of middle precambrian stromatolites. In *Stromatolites* (ed WR Walter), pp. 20, 599–611. Amsterdam: Elsevier.

- Hoffman P** (1976b) Stromatolite morphogenesis in Shark Bay, Western Australia. In *Stromatolites* (ed WR Walter), pp. 20, 261–71. Amsterdam: Elsevier.
- Horodyski RJ** (1977) Lyngbya mats at Laguna Mormona, Baja California, Mexico; comparison with Proterozoic stromatolites. *Journal of Sedimentary Research* **47**, 1305–20.
- Jahnert RJ and Collins LB** (2012) Characteristics, distribution and morphogenesis of subtidal microbial systems in Shark Bay, Australia. *Marine Geology* **306**, 115–36.
- Kah LC, Bartley JK, Frank TD and Lyons TW** (2006) Reconstructing sea-level change from the internal architecture of stromatolite reefs: an example from the Mesoproterozoic Sulky Formation, Dismal Lakes Group, arctic Canada. *Canadian Journal of Earth Sciences* **43**, 653–69.
- Kendall CC, Flood P and Hopley D** (2011) Classification of carbonates. In *Encyclopedia of Modern Coral Reefs* (ed D Hopley), pp. 193–8. Dordrecht: Springer, Encyclopedia of Earth Sciences Series.
- Li Q and Jun YS** (2019) Salinity-induced reduction of interfacial energies and kinetic factors during calcium carbonate nucleation on quartz. *The Journal of Physical Chemistry* **123**, 14319–26.
- Logan BW** (1961) Cryptozoon and associate stromatolites from the Recent, Shark Bay, Western Australia. *The Journal of Geology* **69**, 517–33.
- Logan BW, Rezak R and Ginsburg RN** (1964) Classification and environmental significance of algal stromatolites. *The Journal of Geology* **72**, 68–83.
- Mackey TJ, Sumner DY, Hawes I, Jungblut AD and Andersen DT** (2015) Growth of modern branched columnar stromatolites in Lake Joyce, Antarctica. *Geobiology* **13**, 373–90.
- Marquillas RA** (1984) La Formación Yacoraite (Cretácico Superior) en el río Juramento, Salta: Estratigrafía y ciclicidad. In *IX Congreso Geológico Argentino*, 5–9 November 1984, San Carlos de Bariloche, Argentina, 186–96. Asociación Geológica Argentina.
- Marquillas RA** (1985) Estratigrafía, sedimentología y paleoambientes de la Formación Yacoraite (Cretácico superior) en el tramo austral de la cuenca, Norte Argentino. PhD thesis, Universidad Nacional de Salta. Published thesis.
- Marquillas RA, del Papa C and Sabino I** (2005) Sedimentary aspects and paleoenvironmental evolution of a rift basin: Salta Group (Cretaceous–Paleogene), northwestern Argentina. *International Journal of Earth Sciences* **94**, 94–113.
- Marquillas RA, del Papa C, Sabino I and Heredia J** (2003) Prospección del límite K/T en la cuenca del Noroeste, Argentina. *Revista de la Asociación Geológica Argentina* **58**, 271–4.
- Marquillas RA and Salfity JA** (1989) Distribución regional de los miembros de la Formación Yacoraite (Cretácico Superior) en el noroeste argentino. In *Simposio Cretácico de América Latina, International Geological Correlation Program-Project*, 6–9 June 1989, Buenos Aires, Argentina, 253–72. Asociación Geológica Argentina.
- Marquillas RA and Salfity JA** (1994) Relaciones estratigráficas regionales de la Formación Yacoraite (Cretácico Superior), norte de la Argentina. In *VII Congreso Geológico Chileno*, 17–21 October 1994, Concepción, Chile, **1**, 479–83. Sociedad Geológica de Chile.
- Marquillas RA, Salfity JA, Matthews SJ, Matteini M and Dantas E** (2011) U–Pb zircon age of the Yacoraite Formation and its significance to the Cretaceous–Tertiary boundary in the Salta Basin, Argentina. *Cenozoic Geology of the Central Andes of Argentina* **227–46**.
- Mata SA, Harwood CL, Corsetti FA, Stork NJ, Eilers K, Berelson WM and Spear JR** (2012) Influence of gas production and filament orientation on stromatolite microfabric. *Palaios* **27**, 206–19.
- Mazzullo SJ** (2004) Overview of porosity evolution in carbonate reservoirs. *Kansas Geological Society Bulletin* **79**, 1–19.
- Monty CL** (1976) The origin and development of cryptalgal fabrics. In *Stromatolites* (ed WR Walter), pp. 20, 193–249. Amsterdam: Elsevier.
- Moore LS and Burne RV** (1994) The modern thrombolites of Lake Clifton, western Australia. In *Phanerozoic stromatolites II* (ed J Casanova), pp. 3–29. Dordrecht: Springer.
- Moroni AM** (1984) *Mtchedlishvilia saltenia* n. sp. en sedimentitas del Grupo Salta, provincia de Salta. In *3er Congreso Argentino de Paleontología y Bioestratigrafía*, 6–10 September 1984, Corrientes, Argentina, 129–39. Asociación Paleontológica Argentina and Universidad Nacional del Nordeste (Argentina).
- Nehz O and Woo KS** (2006) The effect of subaerial exposure on the morphology and microstructure of stromatolites in the Cretaceous Sinyangdong Formation, Gyeongsang Supergroup, Korea. *Sedimentology* **53**, 1121–33.
- Palma RM** (1984) Características sedimentológicas y estratigráficas de las Formaciones en el límite Cretácico Superior–Terciario Inferior, en la Cuenca Salteña. PhD thesis, Universidad Nacional de Tucumán. Published thesis.
- Palma RM** (1993) Petrología, ciclos sedimentarios y ambiente depositacional de la Formación Yacoraite (Cretácico Superior) en el río Corralito, Salta. *Información Tecnológica* **48**, 233–40.
- Perissinotto R, Bornman TG, Steyn PP, Miranda NA, Dorrington RA, Matcher GF and Peer N** (2014) Tufa stromatolite ecosystems on the South African south coast. *South African Journal of Science* **110**, 1–8.
- Planavsky N and Grey K** (2008) Stromatolite branching in the Neoproterozoic of the Centralian Superbasin, Australia: an investigation into sedimentary and microbial control of stromatolite morphology. *Geobiology* **6**, 33–45.
- Pratt BR and James NP** (1982) Cryptalgal-metazoan bioherms of early Ordovician age in the St George Group, western Newfoundland. *Sedimentology* **29**, 543–69.
- Preiss WV** (1976) Basic field and laboratory methods for the study of stromatolites. In *Stromatolites* (ed WR Walter), pp. 5–13. Amsterdam: Elsevier.
- Quattrocchio M, Ruiz L and Volkheimer W** (2000) Palynological zonation of the Paleogene of the Colorado and Salta Group basins, Argentina. *Revista Española de Micropaleontología* **32**, 61–78.
- Reid RP and Browne KM** (1991) Intertidal stromatolites in a fringing Holocene reef complex, Bahamas. *Geology* **19**, 15–18.
- Reid RP, James NP, Macintyre IG, Dupraz CP and Burne RV** (2003) Shark Bay stromatolites: microfabrics and reinterpretation of origins. *Facies* **49**, 299.
- Reid RP, Visscher PT, Decho AW, Stolz JF, Bebout BM, Dupraz C, Macintyre IG, Paerl HW, Pinckney JL, Prufert Bebout L, Steepe TF and DesMarais DJ** (2000) The role of microbes in accretion, lamination and early lithification of modern marine stromatolites. *Nature* **406**, 989–92.
- Reitner J, Paul J, Arp G and Hause-Reitner D** (1996) Lake Thetis domal microbialites; a complex framework of calcified biofilms and organominerics (Cervantes, Western Australia). In *Global and Regional Controls on Biogenic Sedimentation I. Reef Evolution. Research Reports* (eds J Reitner, F Neuweiler and F Gunkel), pp. 85–89. Göttingen: Göttinger Arbeiten zur Geologie und Paläontologie.
- Reyes FC** (1972) Correlaciones en el Cretácico de la cuenca Andina de Bolivia, Perú y Chile. *Revista Técnica YPF* **1**, 101–44.
- Riding RE** (2000) Microbial carbonates: the geological record of calcified bacterial algal mats and biofilms. *Sedimentology* **47**, 179–214.
- Riding RE, Awramik SM, Winsborough BM, Griffin KM and Dill RF** (1991) Bahamian giant stromatolites: microbial composition of surface mats. *Geological Magazine* **128**, 227–34.
- Rohrlich V** (1974) Microstructure and microchemistry of Iron Oolites. *Mineralium Deposita* **9**, 133–42.
- Sabino IF** (2002) Geología del Subgrupo Purgua (Cretácico) del noroeste argentino. PhD thesis, Universidad Nacional de Salta. Published thesis.
- Salfity JA** (1980) Estratigrafía de la Formación Lecho (Cretácico) en la cuenca andina del norte argentino. PhD thesis, Universidad Nacional de Salta. Published thesis.
- Salfity JA and Marquillas RA** (1994) Tectonic and sedimentary evolution of the Cretaceous–Eocene Salta Group basin, Argentina. In *Cretaceous Tectonics of the Andes* (ed JA Salfity), pp. 226–315. Wiesbaden: Springer-Verlag.
- Sánchez MC and Marquillas RA** (2010) Facies y ambientes del grupo Salta (Cretácico–Paleógeno) en Tumbaya, Quebrada de Humahuaca, provincia de Jujuy. *Revista de la Asociación Geológica Argentina* **67**, 383–91.
- Sanz-Montero ME, Rodríguez-Aranda JP and Calvo JP** (2005) Biomineralization in relation with endoevaporitic microbial communities. Miocene lake deposits of the Madrid Basin, Central Spain. *Geophysical Research Abstract* **7**, 68–74.
- Sarjeant WAS** (1975) Plant trace fossils. In *The Study of Trace Fossils: A Synthesis of Principles, Problems, and Producers in Ichnology* (ed. RW Frey), pp. 163–79. Amsterdam: Springer Science & Business Media.

- Schneider J** (1977) Carbonate construction and decomposition by epilithic and endolithic micro-organisms in salt-and freshwater. In *Fossil Algae: Recent Results and Developments* (ed E Flügel), pp. 248–60. Amsterdam: Springer.
- Scholle PA** (1978) *A Color Illustrated Guide to Carbonate Rock Constituents, Textures, Cements, and Porosities*. Tulsa: American Association of Petroleum Geologists, 241 p.
- Schopf JW** (1996) Cyanobacteria: pioneers of the early Earth. *Nova Hedwigia Beiheft* **112**, 13–32.
- Schwab K** (1984) Contribución al conocimiento del sector occidental de la cuenca sedimentaria del Grupo Salta (Cretácico-Eogénico) en el noroeste argentino. *Actas* **1**, 586–604.
- Shapiro RS** (2000) A comment on the systematic confusion of thrombolites. *Palaios* **15**, 166–9.
- Shapiro RS and Awramik SM** (2000) Microbialite morphostratigraphy as a tool for correlating Late Cambrian–Early Ordovician sequences. *The Journal of Geology* **108**, 171–80.
- Shinn EA** (1968) Practical significance of birdseye structures in carbonate rocks. *Journal of Sedimentary Petrology* **38**, 215–23.
- Shinn EA** (1983) Birdseyes, fenestrae, shrinkage pores, and loferites; a reevaluation. *Journal of Sedimentary Research* **53**, 619–28.
- Sial AN, Ferreira VP, Toselli AJ, Parada MA, Aceñolaza FG, Pimentel MM and Alonso RN** (2001) Carbon and oxygen isotope compositions of some Upper Cretaceous–Paleocene sequences in Argentina and Chile. *International Geology Review* **43**, 892–909.
- Suárez-González P, Quijada EI, Benito MI and Mas R** (2016) Do stromatolites need tides to trap ooids? Insights from a Cretaceous system of coastal-wetlands. In *Contributions to Modern and Ancient Tidal Sedimentology: Proceedings of the Tidalites 2012 Conference* (eds B Tessier and JY Reynaud), pp. 161–91. USA: John Wiley & Sons.
- Suárez-González P, Quijada IE, Benito MI, Mas R, Merinero R and Riding R** (2014) Origin and significance of lamination in Lower Cretaceous stromatolites and proposal for a quantitative approach. *Sedimentary Geology* **300**, 11–27.
- Suosaari EP, Reid RP, Araujo TA, Playford PE, Holley DK, Mc Namara KJ and Eberli GP** (2016a) Environmental pressures influencing living stromatolites in Hamelin Pool, Shark Bay, Western Australia. *Palaios* **31**, 483–96.
- Suosaari EP, Reid RP, Playford PE, Foster JS, Stolz JF, Casaburi G and Eberli GP** (2016b) New multi-scale perspectives on the stromatolites of Shark Bay, Western Australia. *Scientific Reports* **6**, 57–70.
- Turner JCM** (1959) Estratigrafía del cordón de Escaya y de la sierra de Rinconada (Jujuy). *Revista de la Asociación Geológica Argentina* **13**, 15–39.
- van de Vijzel RC, van Belzen J, Bouma TJ, van der Wal D, Cusseddu V, Purkis SJ, Rietkerk M and van de Koppel J** (2020) Estuarine biofilm patterns: Modern analogues for Precambrian self-organization. *Earth Surface Processes and Landforms* **45**, 1141–54.
- Vennin E, Olivier N, Brayard A, Bour I, Thomazo C, Scarguel G, Fara E, Bylund KG, Jenks JF, Stephen DA and Hofmann R** (2015) Microbial deposits in the aftermath of the end-Permian mass extinction: A diverging case from the Mineral Mountains (Utah, USA). *Sedimentology* **62**, 753–92.
- von der Borch CC** (1974) Stratigraphy of stromatolites occurrences in carbonate lakes of the coorong lagoon area, South Australia. In *Stromatolites* (ed. MR Walter), pp. 413–20. Amsterdam: Elsevier.
- von der Borch CC, Bolton B and Warren JK** (1977) Environmental setting and microstructure of subfossil lithified stromatolites associated with evaporites, Marion Lake, South Australia. *Sedimentology* **24**, 693–708.
- Wacey D, Urosevic L, Saunders M and George AD** (2018) Mineralisation of filamentous cyanobacteria in Lake Thetis stromatolites, Western Australia. *Geobiology* **16**, 203–15.